

# Numerical model to study the valve overlap period in the Wärtsilä 6L 46 four-stroke marine engine

Lamas, M. I., Assoc. Prof.

Rodríguez, C. G., M. Sc.

Rebollido, J. M., Assoc. Prof.

Escola Universitaria Politécnica. Universidade da Coruña, Spain.

## ABSTRACT

*In this paper, a CFD (Computational Fluid Dynamics) analysis was carried out to study the Wärtsilä 6L 46 medium-speed, four-stroke marine engine. For the purpose, the commercial software ANSYS Fluent 6.3 was employed. The aim is to analyze the scavenging of gases, especially during the valve overlap period. Particularly, the pressure, velocity and mass fraction fields were numerically obtained. In order to validate the CFD results, the in-cylinder pressure was successfully compared to experimental measurements for the exhaust, intake and compression strokes of the cylinder operation.*

*This model can be used in future works to improve the performance of these engines because the information provided is very useful to identify regions in which the pressure, velocity or distribution of gases are inadequate. Besides, to compute the quantity of burnt gases which remain inside the cylinder, fresh charge which is expelled through the exhaust valves and study the influence of parameters such as the exhaust and intake pressures, engine speed, cam profile design, etc.*

**Keywords:** Four-stroke engine; computational fluid dynamics (CFD); marine engine

## INTRODUCTION

The compression ignited internal combustion engine (also known as diesel engine) has two main designs, the four-stroke cycle, and the two-stroke cycle. Both are very common in marine applications because of their high efficiency compared with other types of heat engines and the possibility of employing heavy fuel oil, which is a low cost fuel [1]. Merchant ships such as tankers, chemical tankers, bulkcarriers, OBO, container ships, etc, in the power range between 5000 and 15000 kW have recently experienced a change in their tendency. Traditionally, these ships were propelled by two-stroke engines, but nowadays medium-speed (400-600 rpm), four-stroke engines are highly employed in this power range. Fuel consumption have become similar in two and four-stroke engines, and the lower weight, size and cost of four-stroke engines make them very competitive in the market, although the disadvantage of requiring a gear reducer.

In the field of four-stroke marine engines, the Wärtsilä 6L 46 has become very popular on new cruise vessels, bulk carriers, cargo vessels, ferries, fishing boats, tankers, etc since it was launched onto the market in 1988. As the Wärtsilä 6L 46 is a non-reversing engine, in marine applications it is used as auxiliary engine (electric generator) or as main engine connected to a controllable pitch propeller. Some examples of recent applications are the large Spain tuna fish vessels "Albatun 2" and "Panamá Tuna". Other example is the

chemical tanker "Stend Idun" and the cruise vessel "Oasis of the Seas", equipped with six Wärtsilä 46 engines. Due to its high popularity, the Wärtsilä 6L 46 marine engine was chosen to carry out the present work.

For years, the study of the fluid flow inside engines has been mainly supported by experimental tests such as PIV (Particle Image Velocity), LDA (Laser Doppler Anemometry), ICCD cameras, etc. However, in the field of medium and large marine engines, experimental tests are very laborious, expensive, and restricted to a small portion of the whole cylinder, and down-scale models are sometimes not accurate enough. As an alternative solution to experimental techniques, CFD (Computational Fluid Dynamics) has recently become a useful tool to study the fluid flow inside engines. CFD is a branch of fluid mechanics that uses numerical methods and algorithms to analyze problems that involve fluid flows, even complex simulations such as compressible or turbulent flows. Computers are used to perform the calculations by dividing the domain of interest in a large number of sub-domains called mesh or grid. In recent years, CFD has been significantly improved, especially thanks to the performance of computing, allowing more accurate and fast simulations. In the field of engines, CFD is especially useful to design complex components such as combustion chambers, manifolds, injectors or other parameters. Although CFD was integrated in 1960s on the aerospace industry, the first simulations of engines appeared in 1980s. In the last few years, examples of numerical works about

four-stroke engines are those of [2-8], however, they were not applied to medium or large marine engines. Examples of large engines are those of Lamas and Rodríguez [9] and Nakagaya [10], both of them two-stroke type. So far, the field of medium and large four-stroke marine engines has not been investigated extensively enough employing CFD codes. Accordingly, the present paper presents a CFD study of the Wärtsilä 6L 46 four-stroke marine engine. It is the aim of this paper to present results of the flow characteristics inside the cylinder, especially during the valve overlap period, which has a crucial influence on the performance of the engine.

## DESCRIPTION OF THE ENGINE

### Geometry and specifications

A cross section of the Wärtsilä 6L 46 is shown in Fig. 1 and the main technical characteristics are summarized in Table 1. This engine has six cylinders in line, and every cylinder has two inlet and two exhaust valves. The valve follower is of the roller tappet type, where the roller profile is slightly convex for good load distribution. The valve mechanism includes rocker arms working on yokes guided by pins. The Wärtsilä 46 is provided with Spex (Single pipe exhaust) system and with high efficiency turbocharger.

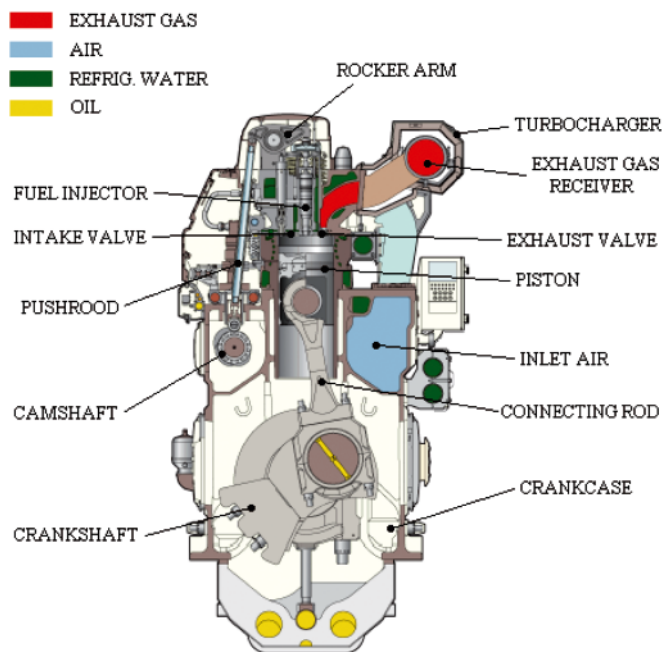


Fig. 1. Cross section. Adapted from Wärtsilä [11]

Tab. 1. Engine specifications at maximum continuous rating

Parameter	Value
Output [kW]	5430
Mean effective pressure [bar]	22.5
Speed [rpm]	500
Cylinder displacement volume [cm <sup>3</sup> /cyl]	96400
Bore [mm]	460
Stroke [mm]	580
Connecting rod length [mm]	1381
Number of cylinders	6
Number of valves per cylinder	2 inlet valves 2 exhaust valves

### Engine operation

Before proceeding with the calculations, the cycle of operation and the valve overlap period will be explained. The principle of operation of a four-stroke engine is as follows. Air is induced into the cylinder by an intake stroke of the piston from TDC (top dead center) to BDC (bottom dead center), thereby increasing the cylinder volume, Fig. 2a. Thus, as the piston moves from TDC to BDC (note that the arrows indicate the direction of the piston), the cylinder is filled with air. After reaching BDC, the piston rises and the intake valves are closed, Fig. 2b. In this compression stroke, the pressure and temperature increases noticeably. A few instants before the piston reaches TDC, the fuel is injected and combustion takes place. After that, the piston descends on the power stroke, Fig. 2c, pushed by the very high pressures caused by the combustion. This pushing force on the piston gives a torque on the crank. After reaching BDC, the products of combustion are expelled through the exhaust valves, Fig. 2d. Finally the piston reaches TDC and the cycle starts again.

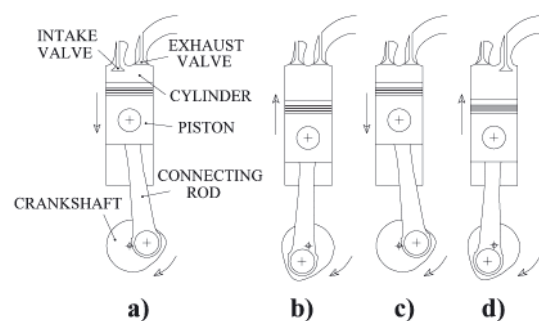


Fig. 2. Engine operation: a) Intake stroke, b) compression stroke, c) power stroke, d) exhaust stroke

Particularly, the valve timing events for the Wärtsilä 6L 46 are shown in Fig. 3. As can be seen, the exhaust valves open 53° before BDC and close 44° after TDC. On the other hand, the intake valves open 50° before TDC and close 26° after BDC.

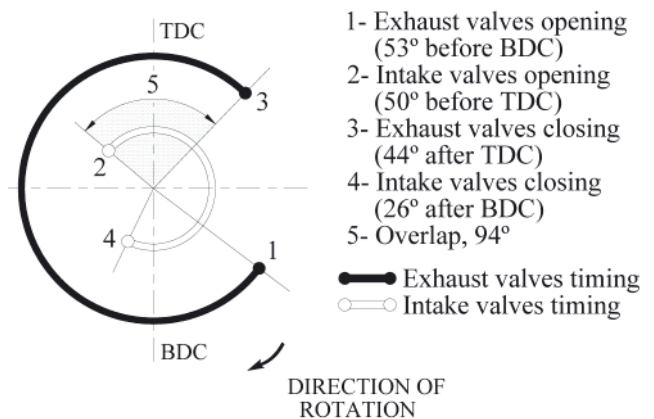


Fig. 3. Valve timing events

As can be seen in Fig. 3, there is a period of 94° between the exhaust and intake strokes when the intake valves are opening and the exhaust valves are closing, i.e., all valves are opened simultaneously. This is called the valve overlap period, and is very important in large four-stroke diesel engines with high turbocharging because the expelling of the burnt gases by the fresh air is more efficient. The overlap period is also useful to refrigerate (the entering air at low temperature refrigerates the walls of the combustion chamber, piston head and exhaust

valves. Besides, this air mixes with the burnt gases, which are directed to the turbocharger turbine. If these gases were too hot, the turbine blades would be damaged).

For these reasons, the overlap period is very necessary. Unfortunately, the potential for mechanical or gas flow mayhem during the overlap period is obvious. If the cylinder and exhaust pressures are too high, large quantities of exhaust gas can be shuttled into the intake tract. This gas is hot, maybe 1000°C, and can cause fuel residues on the back of the intake valves. Besides, if exhaust gas occupies the inlet conduct, only a fraction mass of air can be induced into the cylinder. If the air is not enough, the combustion is incomplete and the consequence is that an excess of unburned hydrocarbon emissions are expelled to the atmosphere. Hence, the design process of the engine during the valve overlap period is a very critical issue. In this regard, CFD is a very useful tool.

### Experimental results

Experimental measurements were carried out by means of several pressure and temperature sensors situated at different parts of a Wärtsilä 6L 46. These measurements were carried out at 96% load and 499.6 rpm. For these conditions, the indicated power was 7153 kW and the consumption was 172 g/kWh (note that this low value of consumption is comparable to a two-stroke engine). The engine performance analyzer MALIN 6000 (Malin Instruments, Ltd.) was employed to obtain the Fig. 4, which represents the in-cylinder gauge pressure versus the position of the piston.

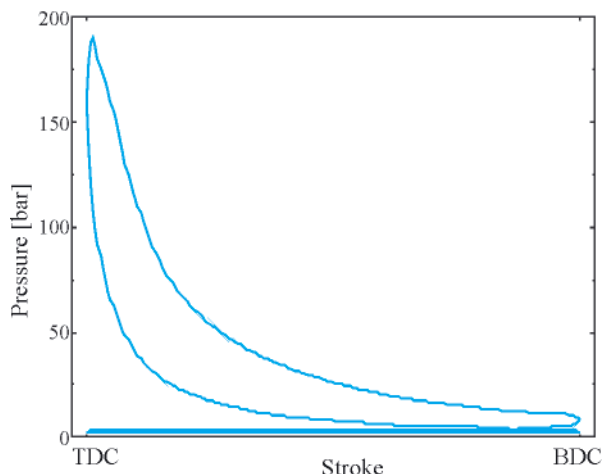


Fig. 4. In-cylinder pressure experimentally measured

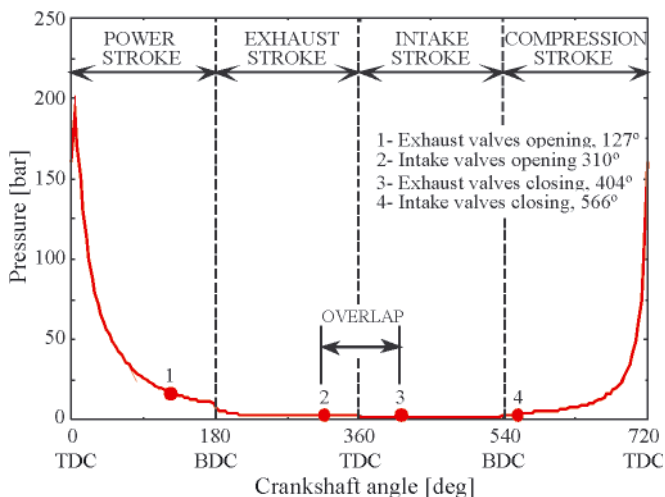


Fig. 5. In-cylinder pressure experimentally measured, opened diagram

In the present paper, the crank angles will be given with reference to the top dead center at the beginning of the power stroke. From this point, the different instants will be referred as this reference position. Accordingly, the opened pressure-crankshaft diagram is shown in Fig. 5. In this reference system, the exhaust valves open at 127° and close at 404° and the intake valves open at 310° and close at 566°. The valve overlap period takes place between 310° and 404°.

Other representative values obtained from the experimental measurements are shown in Table 2.

Tab. 2. Engine test summary.

Parameter	Value
Load [%]	96
Speed [rpm]	499.6
Indicated power [kW]	7154
Maximum pressure [bar]	192
Indicated mean effective pressure [bar]	29.7
Boost pressure [bar]	2.8
Ambient temperature [°C]	25
Intake temperature [°C]	55
Exhaust temperature, before turbocharger [°C]	451
Exhaust temperature, after turbocharger [°C]	350
Exhaust temperature, cylinder [°C]	371

## MUMERICAL PROCEDURE

### Simplifications

As the measurements of all cylinders were practically identical, only one of them was studied. The exhaust, intake and compression strokes were simulated. The combustion stroke is out of range of the present work due to its mathematical complexity. In order to simplify the model, only two components were simulated, air and burnt gases. All actual components could be computed but, since no combustion was simulated, there would not be much difference on the results.

### Governing equations

The governing equations of the turbulent flow inside the cylinder are the RANS (Reynolds-Averaged Navier-Stokes) equations. The energy equation is also needed to compute the thermal problem. Finally, as there are two components (air and burnt gases), one more equation must be added to characterize the mass fraction field. These equations are briefly described in what follows.

In Cartesian tensor form, the continuity equation is given by:

$$\frac{\partial \rho}{\partial t} + \frac{\partial}{\partial x_i} (\rho u_i) = 0 \quad (1)$$

where:

- $u$  – Reynolds average velocity
- $\rho$  – the density.

The flow was considered an ideal gas, so the density is given by the equation of state of ideal gasses:

$$\rho = \frac{p}{RT} \quad (2)$$

The momentum conservation equation can be expressed as:

$$\begin{aligned} \frac{\partial}{\partial t}(\rho u_i) + \frac{\partial}{\partial x_j}(\rho u_i u_j) = \\ = -\frac{\partial p}{\partial x_i} + \frac{\partial \tau_{ij}}{\partial x_j} + \frac{\partial}{\partial x_j}(-\rho \overline{u_i u_j}) \end{aligned} \quad (3)$$

Equations (1) and (3) are called Reynolds-Averaged Navier-Stokes (RANS) equations. They have the same general form as the instantaneous Navier-Stokes equations, with the velocities and other solution variables representing time-averaged values. In Eq. (3),  $u$  denotes the mean velocities,  $u'$  are the turbulence fluctuations about the ensemble average velocity,  $\tau_{ij}$  is the stress tensor and the term  $-\rho \overline{u_i u_j}$  represents the Reynolds stresses (the over bar denotes the averaging process). In this case, the Reynolds stresses were computed using the Boussinesq hypothesis and the  $k-\epsilon$  model. More details of this procedure can be found in [12] and [13]. The  $k-\epsilon$  model was chosen because it is robust, computationally economic and reasonable accurate for a wide range of turbulent flows, including the present study.

Concerning the heat transfer problem, the energy equation is given by the following expression:

$$\begin{aligned} \frac{\partial}{\partial t}(\rho E) + \frac{\partial}{\partial x_i}[u_i(\rho E + p)] = \\ = \frac{\partial}{\partial x_j} \left[ \left( k_t + \frac{C_p \mu_t}{Pr} \right) \frac{\partial T}{\partial x_j} + u_i \tau_{ij} \right] \end{aligned} \quad (4)$$

where:

$E$  – total energy

$k_t$  – the turbulent kinetic energy [12, 13].

Finally, the equation used to characterize the local mass fraction of air is given by:

$$\frac{\partial(\rho Y_{air})}{\partial t} + \nabla \cdot (Y_{air} \rho \vec{V}) = 0 \quad (5)$$

where:

$Y_{air}$  – the mass fraction of the air.

The mass fraction of the burnt gases,  $Y_{gas}$ , is given by the fact that the total mass fraction must sum to unity:

$$Y_{gas} = 1 - Y_{air} \quad (6)$$

### Boundary and initial conditions

The experimentally measured data summarized in Table 2 were used to establish the boundary conditions. An inlet flow of 2.8 bar and 55°C was imposed at the intake ducts. On the other hand, an outlet condition was employed at the exhaust ducts, at 2.4 bar and 371°C.

As the combustion process was not simulated, the start of computation was chosen at 90° crankshaft angle, which takes place after the completion of the combustion. On the other hand, the end of computation was chosen at 630° crankshaft angle, before the beginning of the combustion of the next cycle. It can be seen in Fig. 5 that the in-cylinder gauge pressure at 90° crankshaft angle is 25.9 bar. Unfortunately, the in-cylinder temperatures can not be measured experimentally because a temperature sensor is not fast enough to accurately capture the in-cylinder temperature along the whole cycle, only being possible to measure the inlet and exhaust temperatures, which are practically constant along the cycle. For this reason, the in-cylinder initial temperature was estimated from an adaptation of

the ideal thermodynamic cycle. Details of the procedure can be found in most undergraduate textbooks on internal combustion engines or thermodynamics, so it is not repeated here. The result at 90° crankshaft angle is 1337°C. Concerning the initial velocity, a value of zero was assumed in the exhaust and intake ducts. Nevertheless, in the cylinder, the initial velocity was assumed as the lineal velocity of the piston at 90° crankshaft angle, i.e., 15.5 m/s.

### Computational mesh

The principle of operation of CFD codes is subdividing the domain into a number of smaller, non-overlapping sub-domains. The result is a grid (or mesh) of cells (or elements). In this work, a grid generation program, Gambit 2.4.6, was used to generate the mesh, which is shown in Fig. 6.

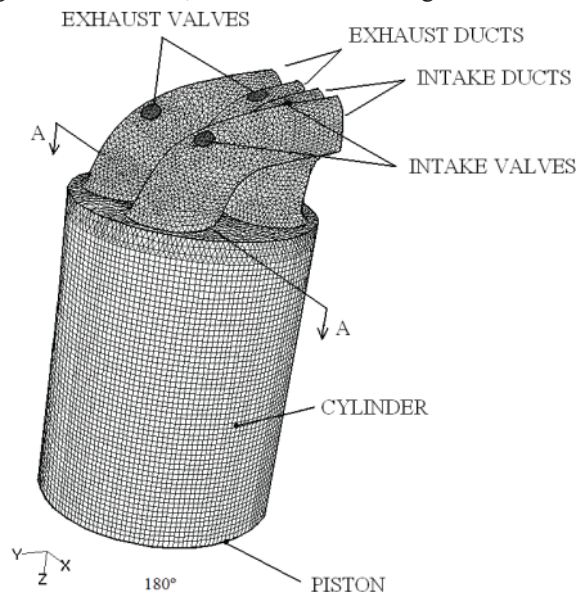


Fig. 6. Computational mesh at 180° crankshaft angle

Due to the movement of the piston and valves, the domain changes into a new position of the calculation and the grid must be automatically reconstruct at each time step. Figure 7 shows the A-A cross section of the mesh at 180° (with the piston at bottom dead center, the intake valves closed and the exhaust

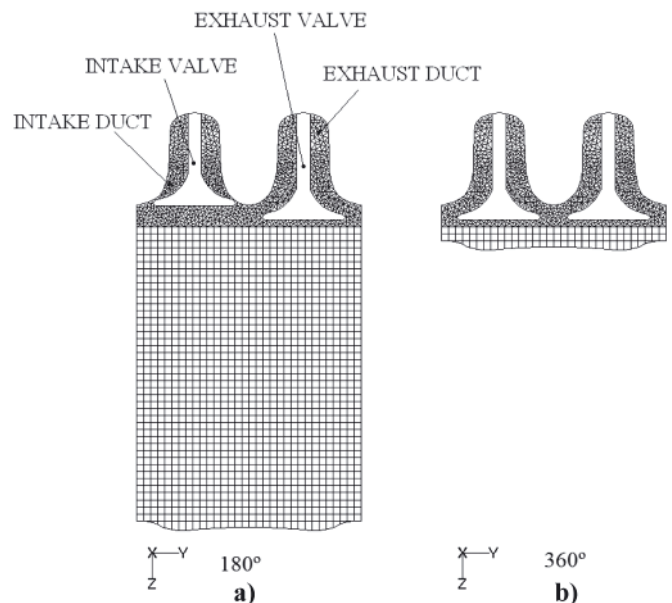


Fig. 7. A-A section of the mesh: a) 180° crankshaft angle, top dead center, b) 360° crankshaft angle, bottom dead center

valves opened) and 360° (with the piston at top dead center, with all valves opened). The number of elements varies from 40000 at top dead center, Fig. 7a to 500000 at bottom dead center, Fig. 7b. In order to minimize the number of cells and obtain good convergence, hexahedral elements were used to mesh the cylinder. Unfortunately, hexahedral elements do not adapt properly to the complex geometry of the valves and ducts, for this reason, tetrahedral elements were employed to the cylinder head and ducts. The cylinder head, especially around valves, was refined in order to capture the complex characteristics of the flow.

### Resolution of the equations

The governing equations were solved using the commercial software Ansys Fluent 6.3, based on the finite volume method. A simple backward Euler scheme was used for the temporal treatment, with a constant time step equivalent to 0.1° crank angle. A second order scheme was chosen for discretization of the continuity, momentum, energy and mass fraction equations, and the PISO algorithm was employed for the pressure-velocity coupling. The computation time was about 4 days in an AMD Phenom II processor with 4 Gb RAM.

## RESULTS AND DISCUSSION

### Validation of the code

In order to ensure that the CFD model is accurate enough, numerical results were compared to experimental measurements in terms of the in-cylinder pressure. For the interval of time studied, from 90° to 630° crankshaft angles, the numerical and experimental results are shown in Fig. 8. Note that an acceptable concordance is obtained between CFD and experimental results, being the average error around 10%.

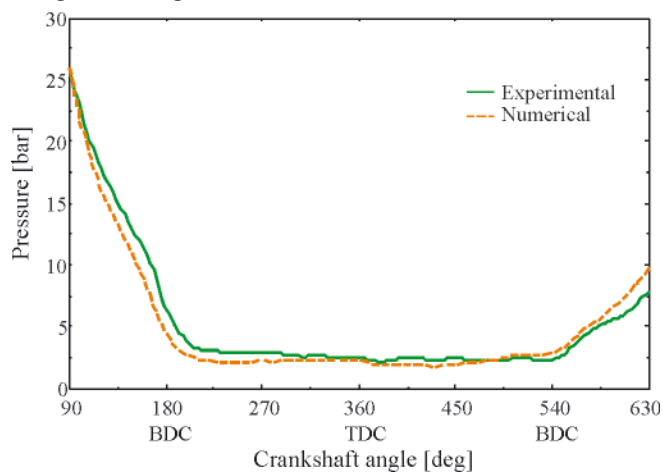


Fig. 8. In-cylinder pressure numerically and experimentally obtained

Figure 9 shows the pressure field on the A-A cutting plane (see Fig. 7) at several crankshaft angles. This plane was chosen in order to appreciate the opening/closing of the exhaust and intake valves. As can be seen, the initial in-cylinder pressure, Fig. 9a is 25.9 bar. At the beginning of the simulation, the pressure descends drastically due to the expansion of the piston. When the exhaust valves are opened, Fig. 9b, the in-cylinder pressure is slightly superior to the exhaust pressure, therefore burnt gasses are expelled through the exhaust ducts. When the intake valves are also opened, Fig. 9c, the in-cylinder pressure has an appropriate value, between the exhaust and intake pressures. Consequently, air enters through the intake ducts and burnt gasses continue being expelled through the exhaust ducts.

Finally, when all valves are closed, the piston is ascending and the gasses are compressed, Fig. 9d.

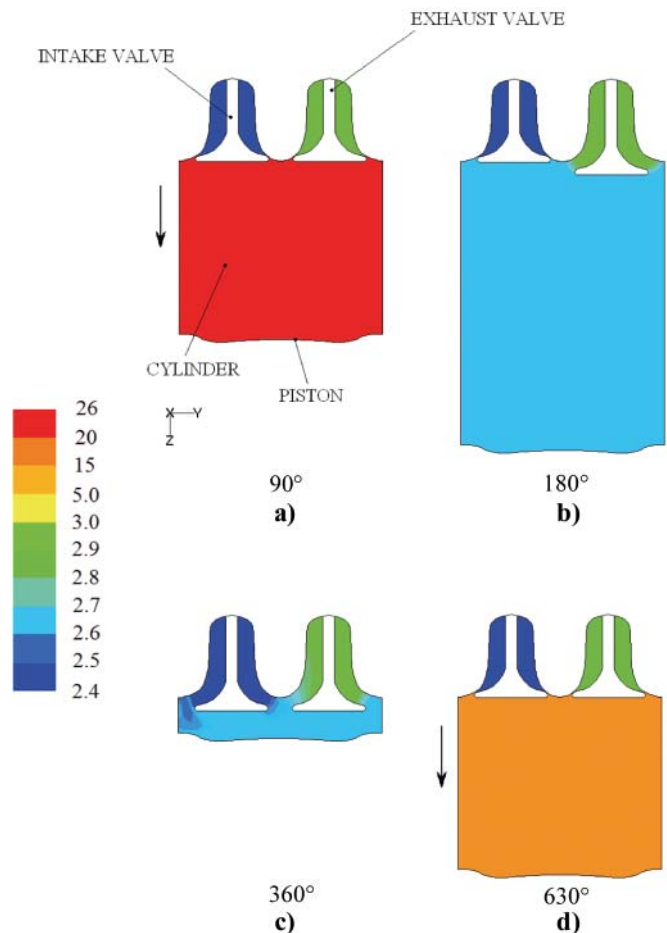


Fig. 9. Pressure field (bar) at several crankshaft angles

### Mass fraction and velocity fields

Figure 10 shows the velocity field overlaid with the pressure field on the A-A cutting plane. As initial conditions, Fig. 10a, the velocity inside the cylinder was imposed as the lineal velocity of the piston and it was assumed that the cylinder and exhaust ducts are full of burnt gasses (red color), while the intake duct is full of air (blue color). When the exhaust valves are opened, Fig. 10b, high velocity burnt gasses are expelled through the exhaust ducts. A short time later, the inlet valves are opened and air enters through the intake ducts and burnt gasses are expelled through the exhaust ducts, Fig. 10c-e. This process of entering fresh air and expelling burnt gasses was verified during all the overlap period, i.e., between 310° and 404°. No retrocession of burnt gasses to the intake ducts was produced. This means that these operating conditions are adequate. Finally, at the end of the simulation, all valves are closed and residual velocities remain into the cylinder.

## CONCLUSIONS AND FURTHER DEVELOPMENTS

In this work, numerical and experimental tests were performed over a commercial four-stroke marine engine, the Wärtsilä 6L 46. A CFD model has been used to simulate the exhaust, intake and compression strokes. Special attention was focused on the overlap valve period, which has a crucial influence on the performance of the engine. It was verified that the fluid flow during the overlap period is correct (no reverse flow was obtained). This work was validated, verifying

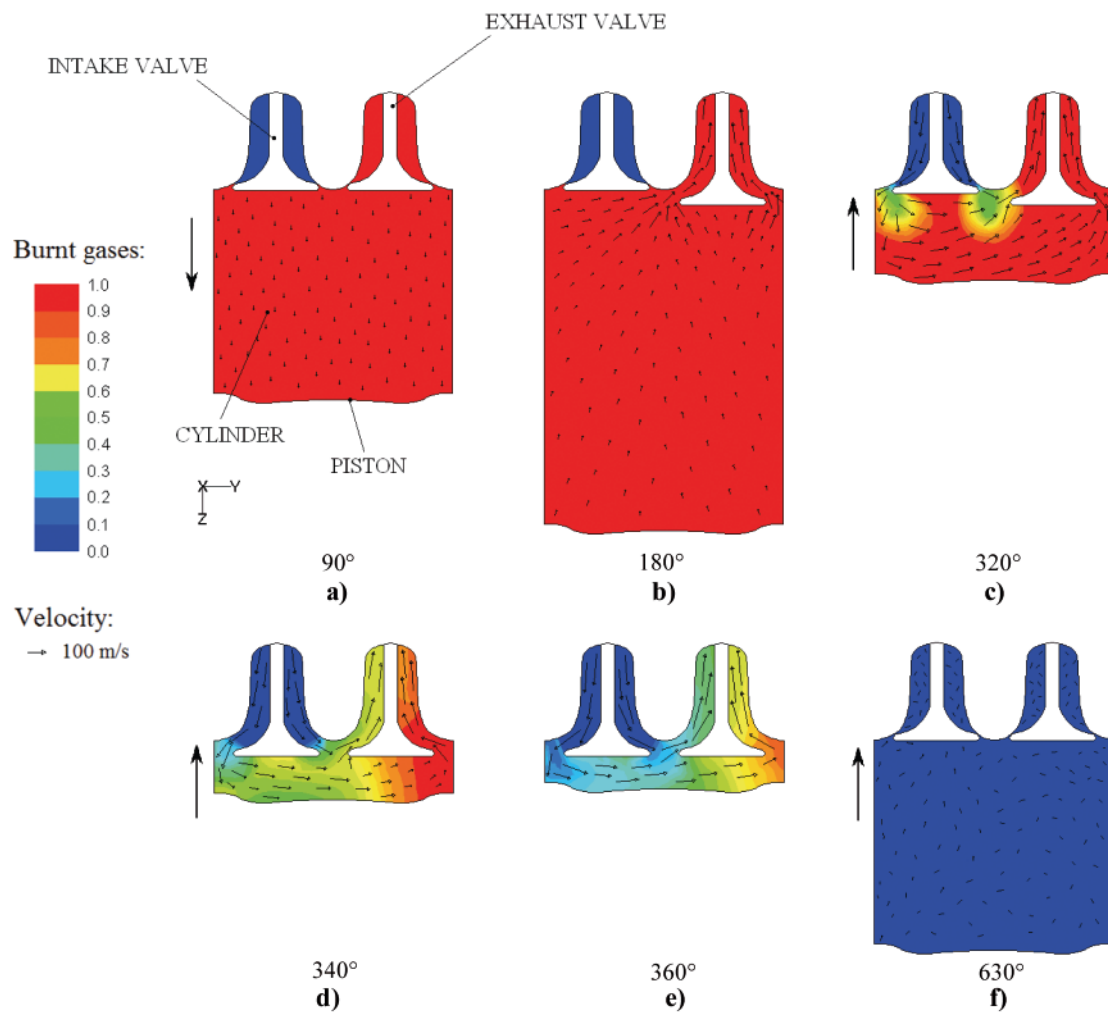


Fig. 10. Velocity field (m/s) overlaid with mass fraction of burnt gases field (-) at several crankshaft angles

that CFD results were in good agreement with experimental measurements of the in-cylinder pressure. This model is an unprecedented opportunity for engineers to understand the highly complex flow interactions that occur in an engine, providing extra information which can not be analyzed with experimental techniques. Besides, this is a very useful tool to improve the performance of the new designs of engines because it is very easy and reasonably cheap to study the influence of parameters such as the exhaust and intake pressures, engine speed, cam profile design, etc.

Although the numerous advantages, it is very important to mention the disadvantages of this CFD procedure. The most important is that it requires high computational resources. For example, the computation time for this problem was four days in an AMD Phenom II processor with 4 Gb RAM memory. Other disadvantage of CFD codes is that the process of generation of the mesh is very delicate. It is very easy to have convergence errors or loose accurate due to an inadequate mesh. In order to obtain good results, it is necessary to make several meshes and ensure that the results are independent of the mesh. Other disadvantage is that some CFD problems are very complicated. In this case, the geometry of the engine, coupled with the complex nature of the motion, in which the valves and piston move, make this a difficult problem to solve.

### Acknowledgements

The authors would like to express their gratitude to “Talleres Pineiro, S.L.”, marine engines maintenance and repair shop.

### NOMENCLATURE

BDC	–	Bottom Dead Center
E	–	energy
g	–	gravity
$k_t$	–	turbulent kinetic energy
p	–	pressure
Pr	–	Prandtl number
R	–	gas constant
t	–	time
T	–	temperature
TDC	–	Top Dead Center
u	–	velocity
Y	–	mass fraction

### Special characters

$\mu$	–	dynamic viscosity
$\mu_t$	–	turbulent viscosity
$\rho$	–	density
$\tau_{ij}$	–	stress tensor

### Subscripts

i	–	Cartesian coordinate (i = 1, 2, 3)
j	–	Cartesian coordinate (j = 1, 2, 3)

### REFERENCES

1. Woodyard, D.: *Pounder's marine diesel engines and gas turbines*. 8<sup>th</sup> Edition. Amsterdam. Elsevier 2004.

2. Milton, B.E.; Behnia, M.; Ellerman, D.M.: *Fuel deposition and re-atomization from fuel/air flows through engine inlet valves*. International Journal of Heat and Fluid Flow, vol. 22, pp. 350-357, 2001.
3. Payri F.; Benajes J.; Margot X.; Gil, A.: *CFD modeling of the in-cylinder flow in direct-injection diesel engines*. Computers & Fluids, vol.33 p.995-1021, 2004.
4. Moureau, V.; Angelberger, C.: *Towards large eddy simulation in internal combustion engines: simulation of a compressed tumble flow*. SAE Paper 011995, 2004.
5. Huang, R.F.; Huang, C.W.; Chang, S.B.; Yang, H.S.; Lin, T.W.; Hsu, W.Y.: *Topological flow evolutions in cylinder of a motored engine during intake and compression strokes*. Journal of Fluids and Structures, vol. 20, pp. 105-127, 2005.
6. Yang, S.L.; Siow, Y.K.; Teo, C.Y.: *A Kiva code with Reynolds-stress model for engine flow simulation*. Journal of Energy Conversion, vol. 30, pp. 427-445, 2005.
7. Semin; Idris, A.; Bakar, R.A.: *Effect of port injection CNG engine using injector nozzle multi holes on air-fuel mixing in combustion chamber*. European Journal of Scientific Research, vol. 34, pp. 16-24, 2009.
8. Ramajo, D. E.; Nigro, N. M.: *In-cylinder flow CFD analysis of a four-valve spark ignition engine: comparison between steady and dynamic tests*. Journal of Engineering for Gas Turbines and Power, vol. 132, 2010.
9. Lamas, M.I.; Rodríguez, C.G.: *CFD analysis of the scavenging process in the MAN B&W 7S50MC two-stroke diesel marine engine*. Submitted to Journal of Ship Research.
10. Nakagawa, H.; Kato, S.; Tateishi, M., Adachi, T., Nakashima, M.: *Airflow in the cylinder of a 2-stroke cycle uniflow scavenging diesel engine during compression stroke*, JSME International Journal, series II, vol. 33, No. 3, pp. 591-598, 1990.
11. Wärtsilä 46. *Project guide for marine applications*. 2001.
12. *Fluent 6.3 Documentation*, 2006. Fluent Inc.
13. Versteeg H K, Malalasekera W.: *An introduction to computational fluid dynamics: the finite volume method*. 2<sup>nd</sup> Edition. Harlow: Pearson Education, 2007.

---

#### CONTACT WITH THE AUTHORS

Lamas M. I., Assoc. Prof.  
 Rodríguez C. G., M. Sc.  
 Rebollido, J. M., Assoc. Prof.  
 Escola Universitaria Politécnica. Universidade da Coruña.  
 Avda. 19 de Febreiro s/n - 15405 Ferrol - A Coruña. SPAIN.  
 e-mail: isabellamas@udc.es